

# Preparation, Characteristics, and Flocculation Behavior of Modified Palygorskite–Polyacrylamide Ionic Hybrids

Meng Wang, Jinwen Qian, Baoqing Zheng, Wuyuan Yang

Department of Polymer Science and Engineering, Zhejiang University, Hangzhou 31002, People's Republic of China

Received 16 June 2003; accepted 5 January 2006

DOI 10.1002/app.24229

Published online in Wiley InterScience (www.interscience.wiley.com).

**ABSTRACT:** A novel inorganic–organic hybrid with modified palygorskite (MPGS) and acrylamide was prepared with a heterogeneous redox initiator system composed of a reductive agent (MPGS) together with an oxidant ( $Ce^{4+}$ ). The MPGS–polyacrylamide (PAM) hybrids were characterized by X-ray diffraction,  $^1H$ -NMR, Fourier transform infrared spectroscopy, conductometry, viscometry, and size exclusion chromatography. The MPGS–PAM hybrid could be a starlike and ionic bond hybrid. The ionization behavior of the MPGS–PAM hybrid in deionized water

depended strongly on its coil dimension and the palygorskite content in the hybrid. The flocculation performance of the MPGS–PAM hybrid in a kaolin suspension was also related to its intrinsic viscosity and the palygorskite content and was better than that of PAM, except for that of the MPGS–PAM hybrid with a high palygorskite content. © 2006 Wiley Periodicals, Inc. *J Appl Polym Sci* 00: 000–000, 2006

**Key words:** water-soluble polymers; clay; solution properties; viscosity; gel permeation chromatography (GPC)

## INTRODUCTION

Recently, many researchers have paid great attention to inorganic–organic polymer hybrids because the addition of inorganic materials to organic polymers endows the polymer materials with many unique physical and chemical properties. Therefore, inorganic–organic polymer hybrids have been used extensively in structural materials,<sup>1,2</sup> electronic and optical materials,<sup>3</sup> and so on. For example, a poly(methyl methacrylate)/sodium montmorillonite hybrid consisting of the silicate clay montmorillonite (MMT) and poly(methyl methacrylate) exhibits a high glass-transition temperature and a high storage modulus.<sup>4</sup> However, the hybrids reported are almost water-insoluble and are used in the solid state. We did a few studies on water-soluble hybrids consisting of inorganic metal ions and organic polymers and used them as flocculants in water treatments.<sup>5,6</sup> In this study, a novel inorganic–organic polymer hybrid with palygorskite (PGS) was prepared and characterized; PGS is a more typical inorganic clay compound compared to inorganic metal ions and also has good adsorption by itself due to its porous structure.<sup>7</sup> Meanwhile, its flocculation performance was explored and also explained from the chain structures of the hybrid.

## EXPERIMENTAL

### Materials

The chemicals used for this study were as follows. A composition of PGS clay (Anhui Guan Shan Mine Co., Jiashan, China) was used. The PGS clay was milled after it was baked at 470°C in a muffle and then sifted out with the sifter (100 holes/in.) before use and was then characterized by X-ray diffraction (XRD). The PGS was composed of magnesium phyllo- $Mg_5(Si_4O_{10})_2(OH)_2(H_2O)_8$  (55.8 wt %), magnesium aluminum phyllo- $(Mg_{0.669}Al_{0.331})_4(Si_4O_{10})_2(OH)_2(H_2O)_8$  (42.2 wt %), and silicon oxide ( $SiO_2$ ; 2.1 wt %). Acrylamide (AM; National Medicines Shanghai Co., reagent grade, Shanghai, China), ethanolamine (Shanghai SSS Reagent Co., Ltd.), ammonium ceric nitrate (Shanghai Yuelong Non-ferrous Metals Co.), and hydrochloric acid, acetone, and sodium chloride (NaCl; Shanghai Chemical Reagent Co.) were also used. The water used in all of the experiments was deionized by a reverse osmosis apparatus (the membrane was purchased from Hydranautics Co., Ocean-side, CA) and purified to a specific conductivity ( $\kappa$ ) of  $0.95 \times 10^{-6}$  S/cm.

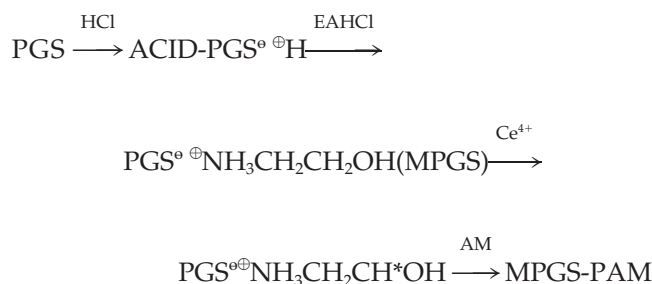
### Preparation of the modified palygorskite (MGPS)–polyacrylamide (PAM) hybrids

The acid activation of PGS was conducted with hydrochloric acid according to the literature.<sup>8</sup> Acid-activated PGS was reacted with ethanolamine hydrochloride (EAHCl) in a flask with a condenser at 70°C for 2 h. The cation  $^+NH_3CH_2CH_2OH$  replaced  $H^+$  and combined with a silicon–oxygen tetrahedron in PGS

Correspondence to: J. W. Qian (qianjw@zju.edu.cn).

Contract grant sponsor: National Natural Science Foundation of China; contract grant number: 50173034.

by electrovalent bonding. The MPGS obtained was washed with deionized water until there was no EAHCl in the filtrate, as measured by a spectrophotometer, and then dried at 50°C. AM was initiated by a heterogeneous redox initiator system composed of the reductive agent MPGS together with the oxidant  $\text{Ce}^{4+}$ , and the MPGS–PAM hybrid was obtained. The process of the reactions was as follows:



The MPGS was dipped and washed more than three times in deionized water to remove the ethanolamine before polymerization.

For comparison, an ionomer of polyacrylamide (iPAM) was prepared by AM and EAHCl without PGS. Also for comparison, a pure PAM was also synthesized via free-radical polymerization initiated with  $\text{NaHSO}_3$ – $(\text{NH}_4)_2\text{S}_2\text{O}_8$  ( $\text{NaHSO}_3 = 7.0 \times 10^{-6}$  mol;  $(\text{NH}_4)_2\text{S}_2\text{O}_8 = 6.5 \times 10^{-6}$  mol; AM = 1.06 mol). All samples of the MPGS–PAM hybrid, iPAM, and PAM were precipitated by acetone and then dipped and washed more than three times in deionized water/acetone and acetone to remove AM monomers and other impurities dissolved in water and dried at 50°C in an oven.

### Specific $\kappa$ measurements

The specific  $\kappa$  in dilute aqueous solution of the hybrid samples was measured by a conductometer (model DDS-11A, Shanghai Rex Instruments Factory, Shanghai, China) at  $30 \pm 0.5^\circ\text{C}$ .

### Viscosity measurements

Aqueous solutions of the samples were prepared at about 45°C for more than 48 h. The reduced viscosity ( $\eta_{sp}$ ) was measured with an Ubbelohde viscometer (Hangzhou Instruments Factory, Hangzhou, China) at  $30 \pm 0.02^\circ\text{C}$ . The flux time was recorded until reproducible values were obtained. The intrinsic viscosity ( $[\eta]$ ) of each sample was determined by an extrapolation procedure from data obtained for various concentrations of solutions, according to the Fuoss equation,<sup>9</sup> which is available to polyelectrolyte aqueous solutions without added salt. The Huggins equation<sup>10</sup> was used to calculate  $[\eta]$  of the pure PAM sample:

**TABLE 1**  
Synthesis of Palygorskite–Polyacrylamide Hybrids

Sample	$C_{\text{MPGS}}$ (wt %)	$C_{\text{PGS}}$ (wt %)	Polymerization time (h)	$[\eta]$ (mL/g)
1	0.06	0.05	36	884
2	0.06	0.05	48	1681
3	3.36	1.92	24	140
4	3.36	1.92	30	535
5	3.34	1.92	36	833
6	3.35	1.85	60	1752
7	0.37	0.34	36	842
8	6.78	5.5	36	823
9	0.00	0.00	8	900

The oxidant in the initiator system was a  $(\text{NH}_4)_2\text{Ce}(\text{NO}_3)_6$  solution (0.1 mol/L) with a medium of 1.0 mol/L  $\text{HNO}_3$ , and the dosage was fixed compared with MPGS.

$$\frac{C}{\eta_{sp}} = \frac{1}{[\eta]} + BC^{1/2} \quad (1)$$

$$\eta_{sp}/C = [\eta] + k_H[\eta]^2C, \quad (2)$$

where  $B$  and  $k_H$  are a constant and Huggins constant, respectively.

### Size exclusion chromatography (SEC)

SEC measurements were carried out at 40°C on a Waters size exclusion chromatograph (Waters Co., Milford, MA) equipped with a Waters 515 High Performance Liquid Chromatography (HPLC) pump and a Waters 2410 refractive-index detector. Poly(ethylene oxide) was used as standard samples for the calibration curve. The eluent was a 0.1 mol/L  $\text{NaNO}_3$  aqueous solutions with a flow rate of 0.8 mL/min.

### Absorbance measurement

The flocculant solution was prepared by the dissolution of the flocculant in water with 0.002 g/mL. For the flocculation test, we used a 100-mL stoppered graduated cylinder and a stopwatch. The 0.5 wt % kaolin suspension was placed in the cylinder, the chemical was added, and the cylinder was inverted 10 times. After mixing, the cylinder was set upright for a residence time of 5 min. Then, the absorbance of supernatant was measured with a spectrophotometer (Spectrophotometer-722, Shanghai Third Analytical Instruments Factory, Shanghai, China). The relative absorbance ( $A_{\text{rel}}$ ) was defined as the ratio of the absorbance of the supernatant and original suspension.

## RESULTS AND DISCUSSION

### Synthesis of the MPGS–PAM hybrid

Table I shows the synthetic details of the MPGS–PAM hybrids. From Table I, prolonging polymerization

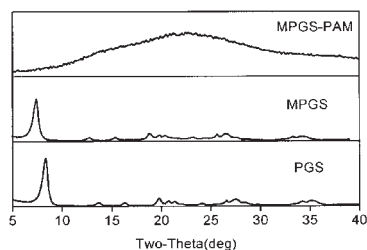


**Figure 1** XRD patterns of the MPGS-PAM hybrid, MPGS, and PGS.

time at a constant dosage of MPGS hybrids (samples 1 and 2 or sample 3–6) produced an elevation in their  $[\eta]$ 's. Obviously, the prominent effect of polymerization time on  $[\eta]$  of the hybrid could be attributed to the polymerization in nonhomogeneous systems. The palygorskite content ( $C_{\text{PGS}}$ ) in the MPGS-PAM hybrid increased greatly with increasing content of modified palygorskite ( $C_{\text{MPGS}}$ ) in the polymerization with a fixed polymerization time of 36 h (samples 1, 5, 7, and 8), but the  $[\eta]$ 's of the hybrids decreased a little. We considered that the free radicals fixed in the channel of MPGS in the nonhomogeneous polymerization system did not diffuse, and only the monomers entered the channel to polymerize. This was greatly different from the free-radical reaction in homogeneous polymerization systems.

### Characterization of the MPGS-PAM hybrid

The XRD patterns of the MPGS-PAM hybrid, MPGS, and PGS, which were obtained by XRD with a D/Max-2550pc X-ray diffractometer (Bruker, Billerica, Germany; 40kv, 300 mA) with Cu  $K\alpha$  ( $\lambda = 0.15406$  nm) radiation. The step width was  $0.02^\circ$  over a range of  $2\theta = 2\text{--}10^\circ$ . The XRD patterns are shown in Figure 1. PGS had a characteristic diffraction peak at  $2\theta = 8.27^\circ$ , on the basis of the Bragg equation, corresponding to a galley spacing of 1.04 nm. MPGS had a characteristic diffraction peak at  $2\theta = 7.38^\circ$ ; the corresponding  $d$ -spacing was 1.17 nm, which was larger than the  $d$ -spacing of PGS. This showed that the  $d$ -spacing of MPGS modified by EAHCl was larger than that of PGS. This indicates that the EAHCl inserted the cavity of the PGS. However, the MPGS-PAM hybrid had no characteristic diffraction peak; this showed that the inorganic started to peel off, and intercalation polymerization occurred.

The MPGS-PAM hybrid was also characterized by NMR and Fourier transform infrared (FTIR) spectroscopy. Figure 2 shows the  $^1\text{H-NMR}$  spectrum of the MPGS-PAM hybrid by an AVANCE DMX500 (Bruker Co., Germany). A new peak at  $\delta = 3.64$  appeared, which represented the H sign of  $\alpha$ -carbon in the  $^+\text{NH}_3$  group of  $\text{NH}_3\text{CH}_2\text{CH}(\text{OH})^-$ . Also, when we com-

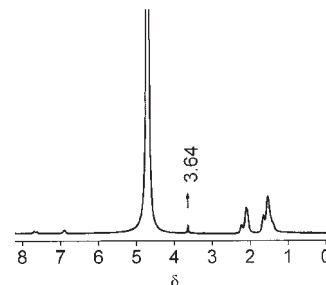


**Figure 2**  $^1\text{H-NMR}$  spectrum of the MPGS-PAM hybrid.

pared the following facts, that the ethanolamine was removed in the reductive agent MPGS before polymerization, the MPGS-PAM hybrid was dissolved in the deionized water very well, and also, the existing PGS component in the MPGS-PAM hybrid was based on the data of thermogravimetry in a muffle  $750^\circ\text{C}$ , we considered that a conjunction between  $\text{O}^-$  and  $^+\text{NH}_3$  in the MPGS or in the MPGS-PAM hybrids did exist. Furthermore, Figure 3 shows the FTIR spectra of the MPGS-PAM hybrid and PAM, which were recorded on VECTOR 22 spectrometer (Bruker) at room temperature. A pair of new peaks  $980$  and  $1031\text{ cm}^{-1}$  in the MPGS-PAM hybrid were revealed, which represented the vibration of  $\text{Si-O-Si}$  and  $\text{Si-O}$  in MPGS.<sup>11</sup>

### $\kappa$ behavior

Figure 4 shows the plots of  $\kappa$  versus the molar concentration ( $C$ ) of the MPGS-PAM hybrid in aqueous solutions at constant  $C_{\text{MPGS}}$  or  $C_{\text{PGS}}$  at  $30^\circ\text{C}$ . The  $\kappa$  values, reflecting the charge number ionized, increased linearly with  $C$  and was positively proportional to  $[\eta]$ . The slope ( $S$ ) of the line, representing the rate of ionization of the hybrid, increased with increasing  $[\eta]$  (or molecular weight) of the MPGS-PAM hy-

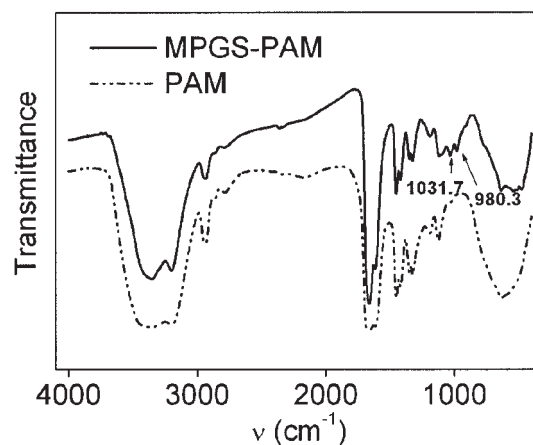


**Figure 3** FTIR spectra of the MPGS-PAM hybrid and PAM.

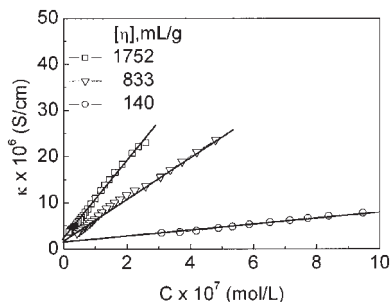


**Figure 4**  $\kappa$  as a function of  $C$  of the hybrids at a constant  $C_{\text{PGS}}$  and at 30°C.

brid. This means that the ionization of the hybrid with high molecular weight was easier than that with low molecular weight. It was very similar to the behavior of simple electrolytes,<sup>12</sup> in which the larger the ion radii is, the smaller the energy of the ion pair and the easier the ionization of the ion pair will be. However, with increasing  $[\eta]$  of the MPGS-PAM hybrids, the intercepts of the lines were almost the same because the intercept or limit conductivity ( $\kappa_0$ ) was equal to the sum of  $\kappa$ 's from the solvent (deionized water) and one MPGS-PAM chain with the charged end group of  $\text{O}^-$  in MPGS and  $\text{NH}_3$  at the end of the PAM chain in the infinite dilute solution.

Figure 5 shows the plots of  $\kappa$  versus  $C$  of the MPGS-PAM hybrids and PAM with close  $[\eta]$ 's in aqueous solutions at 30°C. As shown in Figure 5,  $k$  and  $S$  both increased with increasing  $C_{\text{PGS}}$  in MPGS-PAM hybrids because of the ionization of more ion pairs between MPGS and the PAM chain. Also, the intercepts of the line, or  $\kappa_0$ , were almost the same despite  $C_{\text{PGS}}$ . Clearly, as shown in Figure 5, the  $k$  value of the pure PAM was much lower than that of the MPGS-PAM hybrids with close  $[\eta]$ 's.

### Viscosity behavior

Figure 6 shows the variation of  $\eta_{\text{sp}}/C$  of three MPGS-PAM hybrid samples at 30°C, which covered a wide range of  $[\eta]$ 's of hybrids with a constant  $C_{\text{PGS}}$ . All

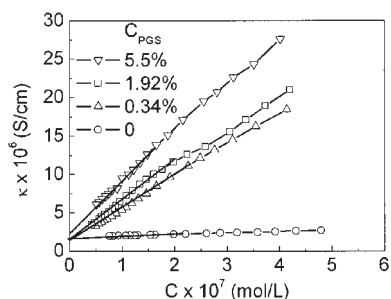


**Figure 5**  $\kappa$  as a function of  $C$  of MPGS-PAM hybrids and PAM at close  $[\eta]$ 's (833, 842, and 823 mL/g at 30°C).

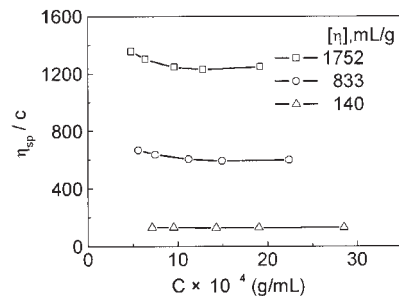


**Figure 6**  $\eta_{\text{sp}}/C$  versus  $C$  for MPGS-PAM hybrids with various  $[\eta]$ 's and at a constant  $C_{\text{PGS}}$  ( $C_{\text{PGS}} = 1.85\text{--}1.92$  wt %) in deionized water.

samples, like the ionomer, showed polyelectrolyte behavior;<sup>13–16</sup> that is, the upturn of the  $\eta_{\text{sp}}/C$  versus  $C$  curve of the hybrid increased with decreasing concentration. Nevertheless, the extent of the upturn increased with increasing  $[\eta]$  of the hybrid. Figure 7 shows the effect of  $C_{\text{PGS}}$  on the  $\eta_{\text{sp}}/C$  versus  $C$  curves of hybrids with close  $[\eta]$ 's. The magnitudes of  $\eta_{\text{sp}}/C$  of both samples were almost equivalent at high concentration, but the steepness of their upturn was greatly different as the concentration decreased. The higher  $C_{\text{PGS}}$  was, the larger the steepness of the upturn was.

### SEC analysis

Figure 8 shows the effect of added salt on the retention time (RT) of the SEC chromatograms of MPGS-PAM2 hybrid. In the presence of 0.1 mol/L  $\text{NaNO}_3$ , RT of the SEC chromatogram was much larger than that without salt, and also, the curve was very smooth. This strong influence was attributed to added  $\text{NaNO}_3$  salt, which weakened the ionization of the hybrid, shielded the interaction of ions, and then decreased the dimension of the hybrid chain. This was consistent with viscosity behavior of the dilute solution, as mentioned previously. SEC traces of the MPGS-PAM2 hybrid and iPAM at different concentrations injected ( $C_i$ 's)

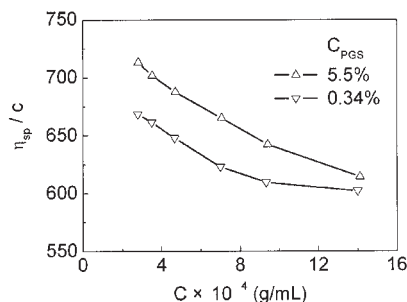


**Figure 7**  $\eta_{\text{sp}}/C$  versus  $C$  for MPGS-PAM hybrids with different  $C_{\text{PGS}}$ 's and at close  $[\eta]$ 's (842 and 823 mL/g at 30°C).

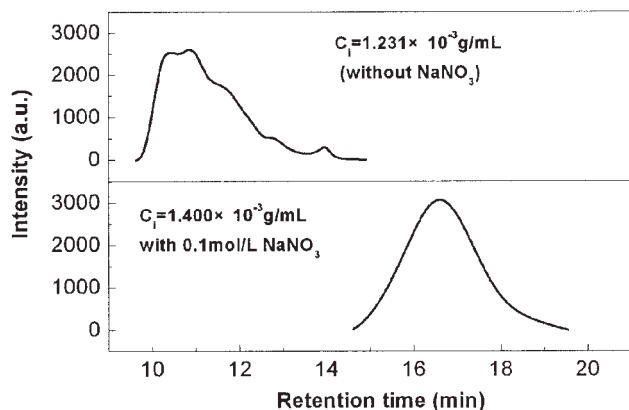


**Figure 8** Comparison of SEC chromatograms of the MPGS-PAM2 hybrid with and without 0.1 mol/L NaNO<sub>3</sub>.

are shown in Figures 9 and 10, respectively. Figure 9 shows three SEC chromatograms of MPGS-PAM2 with different  $C_i$ 's. The roughness of the SEC traces of the MPGS-PAM2 was distinct, especially for the sample with low  $C_i$ . This phenomenon was absent for iPAM (Fig. 10).

Five branching peaks of each SEC chromatogram of two lower  $C_i$ 's ( $C_i = 1.231 \times 10^{-3}$  and  $2.462 \times 10^{-4}$  g/mL) were observed, as shown in Figure 9 (dotted lines), by the fitting of a Gaussian distribution function. Both RT and area ( $A$ ) of each branching peak are listed in Table II. When we compared RT and  $A$  of branching peaks I, II, and III, we observed that the RT values of the three peaks decreased with decreasing  $C_i$ . However, the  $A$  value decreased significantly with decreasing  $C_i$  for branching peaks I and II but increased prominently for branching peaks III. RT of polyelectrolytes decreases with decreasing the solution concentration due to the expansion of chains, such as in Figure 10. Therefore, the decrease in the RT

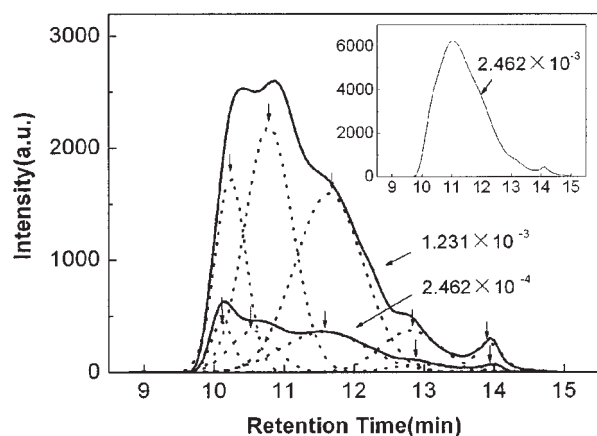


**Figure 9** Effect of  $C_i$  on SEC chromatograms of MPGS-PAM2.  $C_i =$  (1)  $1.231 \times 10^{-3}$  and (2)  $2.462 \times 10^{-4}$  g/mL.

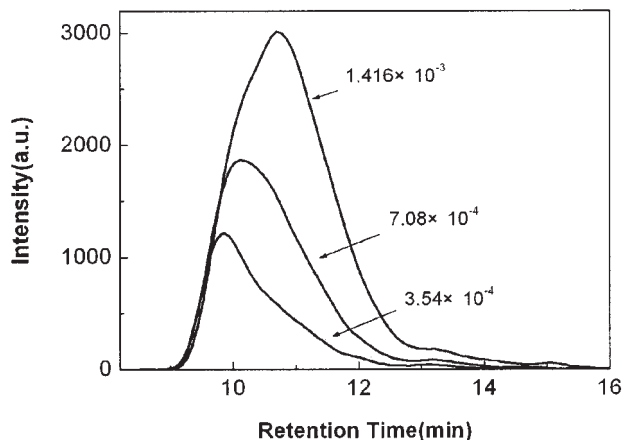


**Figure 10** SEC chromatograms of iPAMs with different  $C_i$ 's.

values of the three peaks was attributed to the expansion of the MPGS-PAM2 chain due to the ionization between  $\text{PGS}^\ominus$  and  $^+\text{NH}_3\text{CH}_2\text{CH}(\text{OH})\text{-PAM}$  in the MPGS-PAM2 with decreasing  $C_i$  from  $C_{i,1}$  to  $C_{i,2}$ . The decrease in  $A$  of peaks I and II were also due to the ionization; that is, the chain numbers (arms) of the MPGS-PAM2 molecules in peaks I and II decreased. Conversely,  $A$  of peak III increased. This led us to consider that peak III represented linear molecules of the MPGS-PAM2 with higher molecular weights compared to those in the peaks IV and V.  $A$  of peak III was the sum of linear MPGS-PAM2 molecules, in which some were from the ionization of the MPGS-PAM2 hybrids with long chain arms in peaks I and II during the dilution.

The preparation process of MPGS-PAM hybrid led us to consider that the conjunction between MPGS and PAM was an ionic bond that was similar to the ionic bonds between MMT silicate and  $-\text{NH}_3^+$  end groups of nylon molecules in nylon-MMT hybrids<sup>2</sup> and also that the chain structure was starlike, in which the PGS

**TABLE II**  
SEC Data of Sample 6 at Different  $C_i$ 's Fitted by a Gaussian Distribution Function

Peak	Peak RT area			
	$C_{i,1} = 1.23 \times 10^{-3}$ g/mL		$C_{i,2} = 2.462 \times 10^{-4}$ g/mL	
	Minutes	%	Minutes	%
Peak I	10.24	18.0	10.11	15.4
Peak II	10.78	34.1	10.55	26.9
Peak III	11.64	38.6	11.58	48.5
Peak IV	12.84	6.9	12.98	6.9
Peak V	13.92	2.4	13.96	2.2
$R^2$	0.9994		0.9984	

particle could have been a core and the chains of PAM acted as arms.

### Flocculation of the MPGS–PAM hybrid

The flocculant performance of the MPGS–PAM hybrid was tested in a 0.25 wt % Kaolin suspension. The results are shown in Figures 11 and 12. In each case,  $A_{rel}$  of the supernatant liquid was plotted against the hybrid concentration (dosage). The lower  $A_{rel}$  was, the better the flocculant performance was. In Figure 11, a series of four MPGS–PAM hybrids with two different  $C_{PGS}$ 's ( $C_{PGS} = 0.05$  and 1.92 wt %) are shown. In both cases, better flocculant performance was displayed in the MPGS–PAM hybrid with higher  $[\eta]$ . The higher  $C_{PGS}$  (1.92) was better than the lower one (0.05) when the  $[\eta]$ 's of the MPGS–PAM hybrids used were close (833 and 884 mL/g). Furthermore, Figure 12 shows the effect of  $C_{PGS}$  (from 0 to 5.5 wt %) on the flocculant performance of various MPGS–PAM hybrids with close  $[\eta]$ 's. The flocculant efficiency increased first and then decreased with increasing  $C_{PGS}$ .

Clearly, the MPGS–PAM hybrid with  $C_{PGS} = 0.335$  wt % gave the best flocculant efficiency. According to the characterization results, the MPGS–PAM hybrid was a type of starlike ionic hybrid; thus, both charge neutralization and bridging mechanisms occurred during the flocculation processes. The starlike structure played an important role, especially in the bridging, and gave better flocculant efficiency compared to PAM. However, the starlike structure was weak and became linearlike due to the polymerization mechanism if more MPGS was added in the synthesis of the MPGS–PAM hybrid. From the chain structure point of view, the starlike MPGS–PAM ionic hybrid was roughly similar to the grafting copolymer of a polyelectrolyte, which also has better flocculant efficiency compared to linear one.<sup>17</sup>

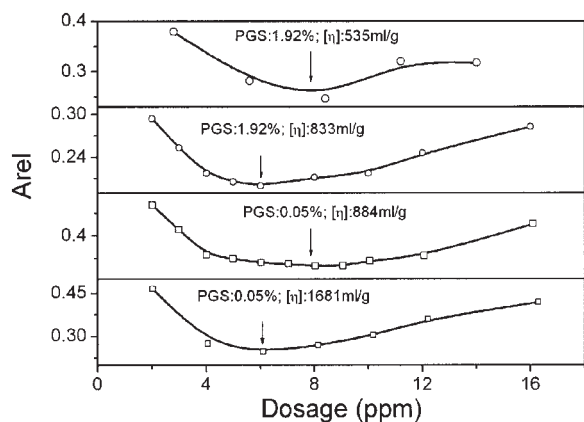


**Figure 11** Effect of  $[\eta]$  of the MPGS–PAM hybrid on the flocculation of the 0.25 wt % kaolin suspension.

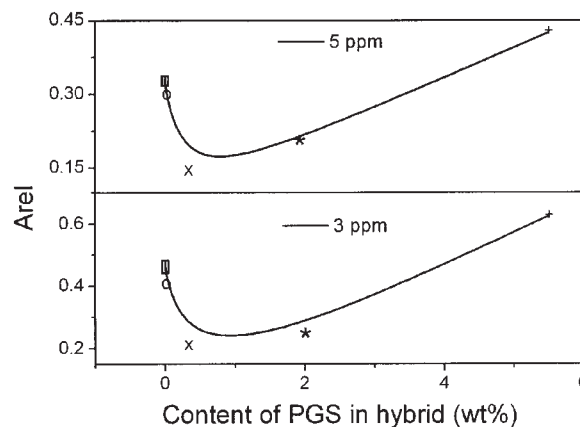


**Figure 12** Effect of  $C_{PGS}$  in the MPGS–PAM hybrid on the flocculation of the 0.25 wt % kaolin suspension.  $C_{PGS}$  (wt %)/ $[\eta]$  (mL/g) of samples: (□) 0/900, (○) 0.05/884, (×) 0.34/842, (\*) 1.92/833, and (+) 5.5/823.

### CONCLUSIONS

A novel inorganic–organic hybrid of MPGS–PAM with MPGS and AM was prepared by a heterogeneous redox initiator system composed of the reductive agent MPGS together with the oxidant  $Ce^{4+}$ . Variation of the preparation parameters resulted in a series of MPGS–PAM hybrids with variation in  $[\eta]$  and  $C_{MPGS}$ . XRD,  $^1H$ -NMR, and FTIR spectroscopy studies of the MPGS–PAM hybrid supported the formation of the hybrid. The study of the  $\kappa$ , viscosity and SEC deduced that the characteristic of the hybrid was starlike and with ionic bonds. From the flocculation experiments, we concluded that the flocculant efficiency of the MPGS–PAM hybrid increased with increasing  $[\eta]$  of the hybrids for the kaolin suspension. At a designed  $[\eta]$ , an optimal  $C_{MPGS}$  existed, at which the hybrid revealed the best flocculation performance. We considered that the chain structure of the starlike hybrid was good for the bridging mechanism. However, more  $C_{MPGS}$ 's in the MPGS–PAM hybrid, due to the addition of more MPGS in the polymerization, resulted in a linear chain in the hybrid.

The authors thank Prof. Xiu-Zhu Xu in department of Chemistry, Zhejiang University for SEC measurements.

### References

- Zoppi, R. A.; de Castro, C. R.; Yoshida, I. V. P.; Nunes, S. P. *Polymer* 1997, 38, 5705.
- Okada, A.; Usuki, A. *Mater Sci Eng C* 1995, 3, 109.
- Kagan, C.; Mitzi, D. B.; Dimitrakopoulos, C. D. *Science* 1999, 286, 945.
- Choi, Y. S.; Choi, M. H.; Wang, K. H.; Kim, S. O.; Kim, Y. K.; Chung, I. J. *Macromolecules* 2001, 46, 8978.

5. Rong, J. F.; Li, H. Q.; Jing, Z. H.; Hong, X. Y.; Sheng, M. *J Appl Polym Sci* 2001, 82, 1829.
6. Yang, W. Y.; Qian, J. W.; Shen, Z. Q. *J Colloid Interface Sci* 2004, 273, 400.
7. Corma, A.; Mifsud, A.; Sanz, E. *Clay Miner* 1987, 22, 225.
8. Suarez Barrios, M.; Flores Gonzalez, L. V.; Vicente Rodriguez, M. A.; Martin Pozas, J. M. *Appl Clay Sci* 1995, 10, 247.
9. Flory, P. J. *Principles of Polymer Chemistry*; Cornell University Press: New York, 1953.
10. Huggins, M. L. *J Am Chem Sci* 1942, 64, 2716.
11. Frost, R. L.; Locos, O. B.; Ruan, H. D. et al. *Vib Spectrosc* 2001, 27, 1.
12. Huheey, J. E. *Inorganic Chemistry: Principles of Structure and Reactivity*, 3rd ed.; American Chemical Society: Cambridge, MA, 1983.
13. Wu, J.; Wang, Y.; Hara, M.; Granville, M.; Jerome, R. J. *Macromolecules* 1994, 27, 1195.
14. Hara, M.; Wu, J.; Lee, A. H. *Macromolecules* 1988, 21, 2214.
15. Peiffer, D. G.; Lundberg, R. D. *J Polym Sci Polym Chem* 1984, 22, 1757.
16. Lundberg, R. D.; Phillips, R. R. *J Polym Sci Polym Phys* 1980, 20, 1143.
17. Tripathy, T.; Karmakar, N. C.; Singh, R. P. *J Appl Polym Sci* 2001, 82, 375.